



# Pre-characterization of a rhodium (111) single crystal for oxidation kinetics experiments

Katja Kustura, University of Zagreb, Croatia

September 10, 2014

## Abstract

This report summarizes the project done in the DESY Nanolab as a part of DESY Summer Student Program. Rhodium single crystal surface was treated by cleaning procedures and characterized by different techniques as a part of its preparation for further oxidation experiments, whose goal is to obtain data needed for future oxidation kinetics studies of rhodium nanoparticles. The sample surface was cleaned by sputtering and annealing, and examined by low electron diffraction, Auger electron spectroscopy, x-ray reflectivity and atomic force microscopy. Although obtained from the manufacturer as a sample ready for experiments, characterization showed contamination by foreign atoms, which was dealt with by sputtering and annealing, and high roughness, which could not be handled during the program. Until the roughness is lowered by further procedures of high temperature annealing, this crystal should not be used in experiments, as the occurrence of any kinds of defects on the surface could significantly alter the course of the experiment and not produce the desired results.

## Contents

<b>I</b>	<b>Introduction</b>	<b>2</b>
I	Motivation for oxidation experiments . . . . .	2
II	Rhodium (111) single crystal . . . . .	2
<b>II</b>	<b>Methods of crystal preparation and characterization</b>	<b>3</b>
I	Sputtering and annealing . . . . .	3
II	Low energy electron diffraction (LEED) . . . . .	3
III	Auger electron spectroscopy (AES) . . . . .	4
IV	X-ray reflectivity (XRR) . . . . .	5
V	Atomic force microscopy (AFM) . . . . .	6
<b>III</b>	<b>Experimental setup and measurement</b>	<b>6</b>
<b>IV</b>	<b>Results and discussion</b>	<b>7</b>
I	LEED patterns and Auger spectra . . . . .	7
II	XRR analysis of the sample . . . . .	9
III	AFM images . . . . .	10
<b>V</b>	<b>Conclusion</b>	<b>10</b>

## I Introduction

### I Motivation for oxidation experiments

The purpose of this project was to prepare rhodium (111) surface for oxidation experiments. Main goal is to in the future study oxidation kinetics of rhodium nanoparticles, and the oxidation analysis of a pure rhodium crystal is the starting point in this study.

Nanoparticles represent "mezzo-scale" between bulk material and atomic structure. Their dimensions range from a few to 100 nm. This is a size range where properties are not independent of size anymore, where surface-area-to-volume ratio increases and surface atoms become dominant, as well as the scale of moving from classical to quantum realm.

All these properties make the study of nanoparticles an area of growing importance due to a vast variety of potential applications that range from chemical engineering and nanocatalysis, over renewable energy technologies such as fuel cells and batteries to nanoelectronics. [1]

Although mostly studied in vacuum, increasing significance of nanoparticles in numerous fields demands a detailed study on how they behave at higher pressures, i.e. normal conditions. Oxidation kinetics experiments are therefore a particularly important step in further understanding and application of nanoparticles and their properties.

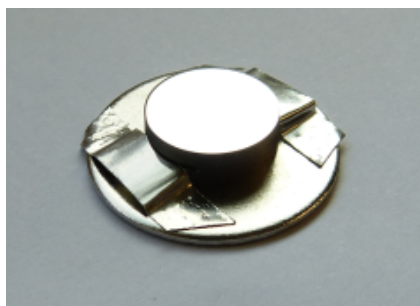


Figure 1: Our rhodium sample

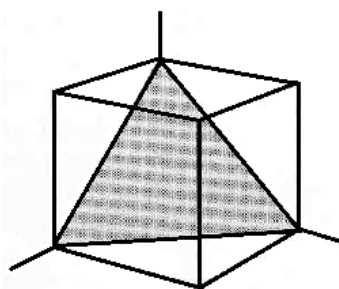


Figure 2: (111) cut (from [2])

## II Rhodium (111) single crystal

Rhodium is a chemical element with chemical symbol Rh and atomic number 45. It is a silvery white transition metal, and is considered both noble and precious, which means it is inert and highly resistant to corrosion and oxidation, as well as very rare. It has outstanding catalytic properties and is primarily used as a catalytic converter in automotive industry, and as a catalyst in chemical industry. Due to its rarity, it is often alloyed with platinum or palladium. The Rh sample used in this project is shown in figure 1.

Crystal structure of Rh is face centered cubic (FCC). Bulk crystal can be cut in various directions and, while the inner structure is always FCC, cutting direction determines the surface structure. This is denoted by the index of plane next to chemical symbol. In our case, the sample studied was Rh(111), which means that the surface was cut along the plane defined by points of the unit cell (1,0,0), (0,1,0) and (0,0,1). Direction of (111) plane with respect to unit cell is shown in figure 2. This cutting direction gives rise to 6-fold symmetry of the surface.

What we are ultimately interested in is the oxidation of Rh nanoparticles, but in order to fully understand it, one should first have a detailed study of a single crystal oxidation. This way it is

possible to distinguish the effects introduced by a nanoparticle system from those already existing for a uniform flat crystal.

Rh(111) single crystal obtained from the manufacturer is already well polished, but it is often the case that the experiments demand even higher degree of flatness and uniformity. The reason for this is that the small defects, in forms of significant surface roughness, microscopic scratches or steps caused by bad cutting, become the centers of the highest activity, due to the high energy stored in the defects. This makes the experiment questionable since it is not clear anymore whether what is observed is due to the defects or due to the flat surface itself.

It is therefore of utter importance to thoroughly go through a number of cycles of preparation and cleaning in order to minimize all the defects and make the surface as flat as possible. This was the aim of this project. Using various techniques, Rh(111) sample was examined and prepared for further experiments.

## II Methods of crystal preparation and characterization

The sample was treated with sputtering and annealing in order to clean the surface from adsorbed impurities and defects. It was then studied with low energy electron diffraction and Auger electron spectroscopy, X-ray reflectivity and atomic force microscopy. In the next few subsections these methods are briefly described.

### I Sputtering and annealing

Sputtering and annealing are two complementary methods for preparing and cleaning the crystal surfaces, both done in the ultra high vacuum chamber (UHV). Sputtering is a process of bombarding the sample with ionized gas, in our case argon, coming from the sputter gun in form of an energetic beam of ionized atoms. By this procedure the surface of the sample is cleaned because it gets hit by ions at high speeds, which enables the removal of contaminants and adsorbed impurities. The sample is sputtered for about 30-45 minutes. Although well suited for cleaning the sample from impurities, sputtering is a highly eroding method in which the surface is damaged.

To flatten the surface after sputtering, annealing is applied. This is simply a heating procedure, in which the sample is heated to temperatures ranging from 800 to 1500 K. The sample is left at high temperature for about 60 minutes. During this period flatness of the surface is restored by thermal movement of surface atoms around the surface, until flat and uniform distribution is achieved. High temperature activates diffusion of bulk impurities to the surface of the sample, which means that the whole procedure of sputtering and annealing has to be repeated many times, until the optimal purity and flatness are achieved.

### II Low energy electron diffraction (LEED)

In order to examine the level of purity of the surface after annealing and sputtering, another two techniques are used: low energy electron diffraction (LEED) and Auger electron spectroscopy (AES).

LEED is a widely used technique for examining quality of a prepared surface. It is based on the diffraction of an electron beam from the surface and is very similar to x-ray diffraction, with a big difference that the mean free path of an electron penetration into the material ( $\sim \text{\AA}$ ) is much smaller than the mean free path of x-rays penetration ( $\sim \mu\text{m}$ ), which makes LEED highly sensitive to surface structures. [3] Electron beam used in LEED has energies ranging from 50 to 400 eV, which corresponds to de Broglie wavelengths of 1.73 to 0.61  $\text{\AA}$ , which further corresponds to atomic

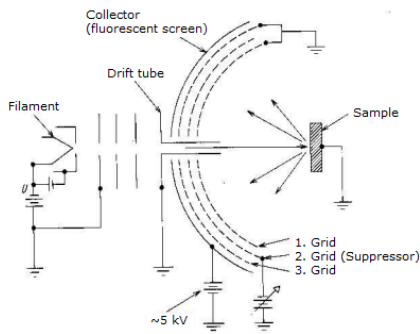


**Figure 3:** LEED display system (from [3])

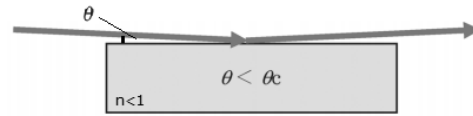


**Figure 4:** X-ray total external reflection (from [6])

dimensions. This is the reason why LEED is a good technique for studying interatomic distances and atomic distributions on the surfaces.

Setup for LEED experiment consists of an electron gun, sample and the hemispherical fluorescent screen, as shown in fig. 3. Electrons hitting the sample scatter under different angles and the constructive interference occurs when the angle of scattering is  $n\lambda = d \sin \theta$ , where  $\lambda$  is the electron wavelength,  $d$  is interatomic spacing (unit cell dimension) and  $\theta$  is the scattering angle. This condition has to be satisfied in both directions at the surface. Constructive interference appears on the screen as bright spots. It is evident that by increasing the energy of the beam, the first order interference occurs under smaller angle and one can see more spots on the screen. Also, the pattern on the screen is an image of reciprocal space - the spacings between the dots get smaller as the interatomic distance increases, and vice versa.

LEED patterns can be quantitatively analysed to obtain information on atomic spacing, surface unit cells or the crystal structure of possible adsorbents on the surface, but it can also be used for a qualitative analysis to determine the purity of the sample. If the surface is clean and flat, LEED pattern will be sharp and symmetrical, with the symmetry mimicking the symmetry of the surface. If, on the other hand, there is an additional structure on the surface, be it crystalline or without particular symmetry, it can be detected on the LEED pattern as new diffraction peaks or as bluntness of the original peaks. This is the way in which LEED was used in this project.

### III Auger electron spectroscopy (AES)

If foreign adsorbates do not change symmetry of the surface, they can not be detected in LEED experiments. For this reason another technique is employed to examine purity of the surface: Auger electron spectroscopy. This is a method in which the sample is again hit by an electron beam, but this time of much higher energy (up to  $\sim 50$  keV). We are interested in excitations of electrons inside an atom, caused by the incident electron beam.

What happens is that the electrons from the beam collide with the atoms at the surface and transfer their energy to the inner atoms, causing ionization. Both the core electron (usually from the K or L shell) and the primary beam electron leave the atom. The remaining gap in the atom is filled by one of the excited electrons jumping to the lower shell. Its energy is either emitted in form of an x-ray photon, or transferred to another, secondary electron in the upper shell. The latter process is called Auger effect and is the key part of AES. [4]

When the secondary electron leaves the atom, it can be detected and its energy measured. Since this energy only depends on the energy levels spacings in the atom, and not on the primary electron beam energy, this method is highly sensitive to types of atoms in the sample. One element can have

many Auger peaks, since they depend on the energy of the core electron and the secondary electron, and these are not firmly specified by the primary beam energy. But the peaks are always specific to a single element and therefore enable us to determine the presence of different atoms on the sample surface.

There exists a database of Auger peaks for each element, which can be used for comparison with the measurement to obtain information on elements on the surface. Again as for LEED, electrons have very short mean free path in the material, which makes AES surface sensitive technique. For practical reasons, instead of measuring number of electrons in dependence on energy, AES is usually done in a derivative mode ( $dN/dE$ ).

#### IV X-ray reflectivity (XRR)

XRR is another surface sensitive technique used most commonly to examine thin layers deposited on a surface. By XRR one can determine thickness of a layer (or multiple layers), roughness of a layer and surface and electron density profile. The idea of XRR is to illuminate the sample with x-rays and measure intensity in the specular direction (reflected angle equal to the incident angle). Impurities on the surface, roughness and other imperfections scatter light in different directions making the reflected intensity deviate from the simple Fresnel reflectivity. These changes can be analysed to get valuable information on surface geometry.

X-rays have index of refraction smaller than unity, giving rise to a total external reflection phenomenon. TER is analogous to total internal reflection occurring at visible wavelengths for higher indices of refraction. Index of refraction of x-rays can be written as  $n = 1 - \delta$ , where  $\delta = \frac{\rho r_0 \lambda^2}{2\pi}$ , with  $\rho$  being the electron density of the material,  $r_0$  the scattering amplitude and  $\lambda$  the wavelength of x-ray. [5] For angles small enough, x-ray coming at the interface with the denser medium will be totally reflected into the first medium (usually air,  $n = 1$ ). The critical angle can be easily derived from the Snell's law:  $\theta_c = \sqrt{2\delta}$ , where the small angle expansion was used and the angle is measured with respect to the surface (fig. 4). [5]

This means that x-rays will have very high specular reflectivity at small angles due to TER, decreasing rapidly at angles  $\theta > \theta_c$ , depending on the absorption of the material, which is introduced as an imaginary part of the refraction index:  $n = 1 - \delta + i\beta$ . Introducing surface roughness or additional layers changes the reflectivity curve, as shown in fig. 5.

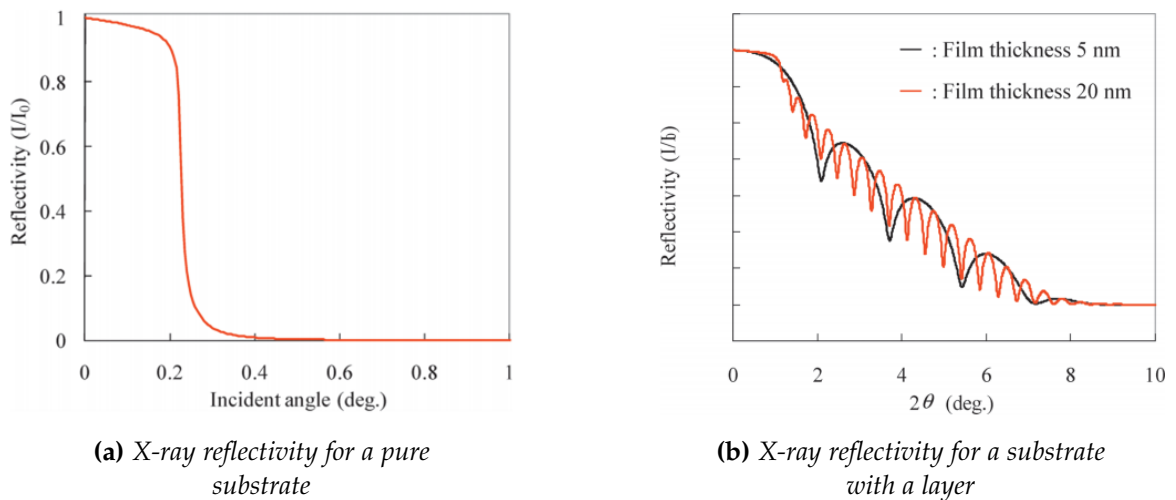


Figure 5: X-ray reflectivity (from [6])

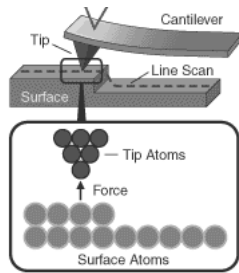


Figure 6: AFM schematic view (from [7])

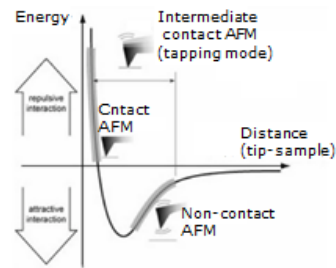


Figure 7: Different modes of AFM (from [8])

## V Atomic force microscopy (AFM)

AFM is an imaging technique used for scanning the surface of the sample. As the name suggests, imaging is based on measuring the force between the sample and the nanotip of the microscope. We know that the atoms interact with each other by Van der Waals forces, so by measuring direction and amplitude of the sample-tip interaction, the distance between them can be determined. By scanning over the surface of the sample, one can obtain topography profile of the sample.

Since the atomic forces are of the order of pN, AFM is a very sensitive technique and the setup has to be well isolated from background and any source of vibrations (sound, electronics, etc.). The size of the tip is of the order of few nm, which determines the resolution of the imaging. Schematic representation of AFM imaging is given in the fig. 6.

AFM can operate in three modes: contact, non-contact and tapping mode. In fig. 7 Lennard-Jones potential is shown, with each mode corresponding to one part of the curve. In this project tapping mode was used to scan and image the surface of our sample.

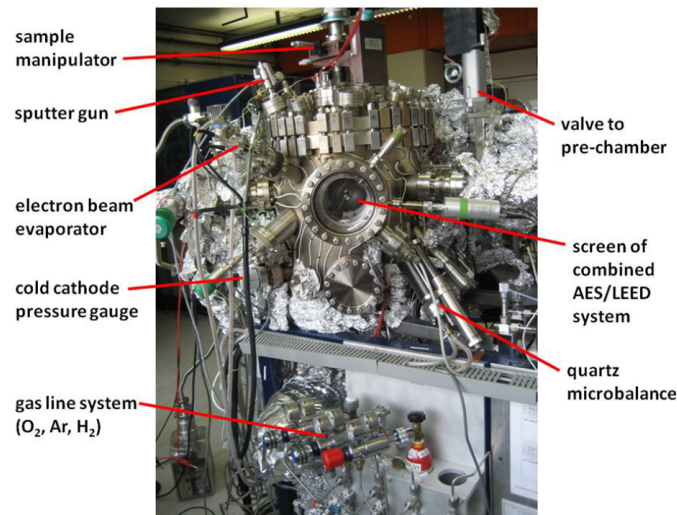


Figure 8: UHV main chamber

## III Experimental setup and measurement

The sample was first loaded into the UHV and transferred to the main chamber. Here all the cycles of sputtering and annealing were done, as well as LEED and AES measurements. The chamber is

shown in fig. 8, together with all the main parts. Sputtering was done by introducing Ar ionized gas into the chamber at the room temperature and the voltage of 1000 V. The pressure due to Ar ionized gas increased up to  $10^{-6}$  mbar. Annealing was done by first pumping the Ar gas out of the chamber and lowering pressure down to  $10^{-10}$  mbar, and then heating the station with the sample by increasing the filament current up to 8.5 A, corresponding to the temperature of 650 °C.

After each cycle of sputtering and annealing, LEED and AES were performed by using the electron gun. Both methods were controlled and configured by RFA (Retarding Field Analyser). LEED patterns were recorded with a camera, and AES spectra were recorded by the program. One Auger spectrum needed about one hour to be recorded.

The sample was then transferred from the UHV to X-ray laboratory where XRR measurements were performed. XRR setup is shown in fig. 9. X-ray source is stationary and the beam is always parallel to the ground. What is rotated are the sample and the detector, in a way that the angles with respect to the ground are always  $\theta$  and  $2\theta$ . Intensity is measured by photon count in the detector. Obtained data was analysed in Fewlay and Origin.



Figure 9: X-ray reflectivity setup

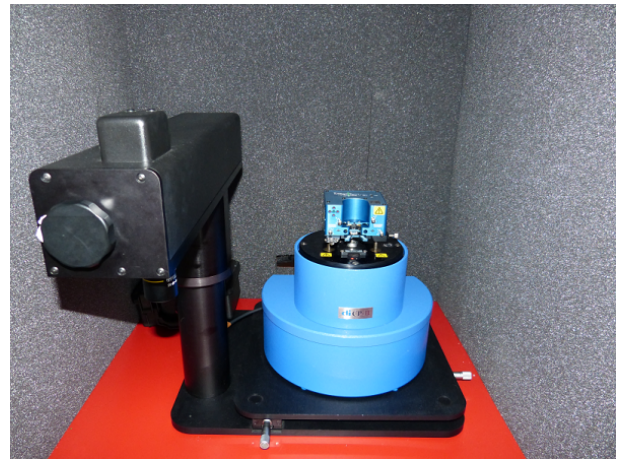


Figure 10: AFM setup

AFM setup is shown in fig. 10. It consists of acoustically isolated scanner and the software for configuring the measurements and taking images. Imaging was handled by The MultiMode SPM unit. Apart from topography, phase measurements were done as well, which give some additional information, like presence of another material on the surface, which can not be detected in topography. Obtained images were analysed in the image editor.

## IV Results and discussion

### I LEED patterns and Auger spectra

LEED patterns for different incident beam energies, before cleaning, are shown in fig. 11. 6-fold symmetry is obvious, which confirms the Rh(111) cut, but the diffraction spots are not sharp. This is an indication of impurities and imperfection of the surface, which make the diffraction peaks blurry. For a more detailed study of the impurities on the surface, AES is to be performed.

Auger spectrum is shown in fig. 12. Comparing it with the Rh reference spectrum (fig. 13), one can see additional peaks, indicating the presence of foreign atoms. Looking up the other Auger reference spectra, we see that these peaks arise from oxygen and carbon atoms. This is hardly

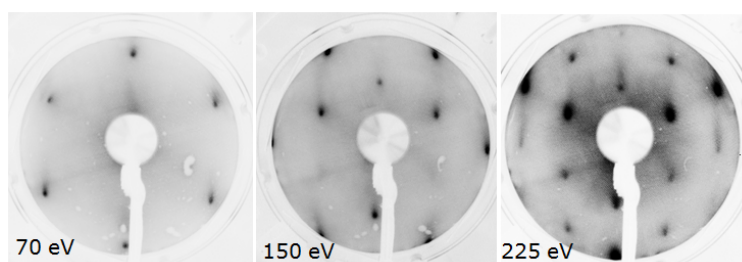


**Figure 11:** LEED patterns before cleaning

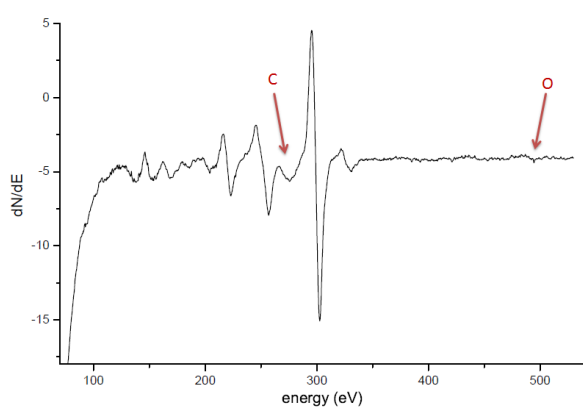


**Figure 12:** Auger spectrum before cleaning

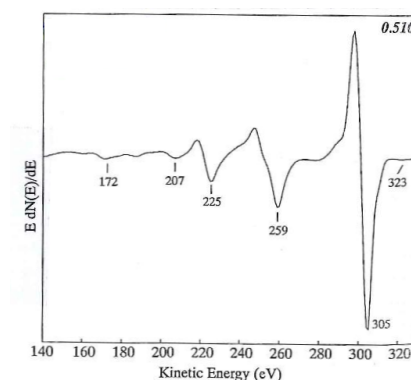


**Figure 13:** Reference Rh Auger spectrum (from Nanolab book)

surprising since these are the most common elements that could occur in normal conditions to which the sample was exposed the whole time prior to its transport to UHV.

Impurities detected by LEED and AES were treated in 4 cycles of sputtering and annealing. Additionally, oxidation was performed as well. This is a treatment in which the chamber is filled with oxygen and annealed. The purpose of this is to enable transport of carbon atoms from the surface in form of carbon dioxide. Afterwards the chamber is vacuumed again and all the oxygen and carbon dioxide are pumped out. After the oxidation, sputtering and annealing have to be performed again to clean the sample from the oxide layer formed during oxidation.

LEED patterns and Auger spectrum after 4 cycles of cleaning and sputtering are shown in figures 14 and 15. From the Auger spectrum we can see that the peaks corresponding to oxygen and carbon disappeared, so the cleaning of the sample from foreign atoms was successful. On the other hand, the LEED pattern is still blurry. Since the surface is cleaned from impurities, this can only be due to high roughness of the sample, which means that annealing did not achieve the desired level of uniformity and flatness.

The problem is that the sample was mounted on an inconel sample holder, which is not applicable at higher temperatures. This is why the highest applied temperature during annealing was around 700 °C. To achieve smaller roughness, the sample should be heated to much higher temperatures (cca. 1200 °C) to raise the mobility of surface atoms. This is achievable by replacing the inconel holder with the molybdenum one, which can endure much higher temperatures. While this project was being carried out, repeating annealing at higher temperatures was not possible due to technical problems with the UHV chamber.

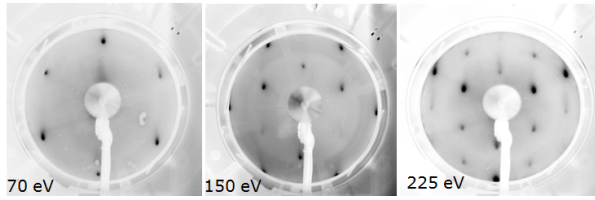


Figure 14: LEED pattern after cleaning

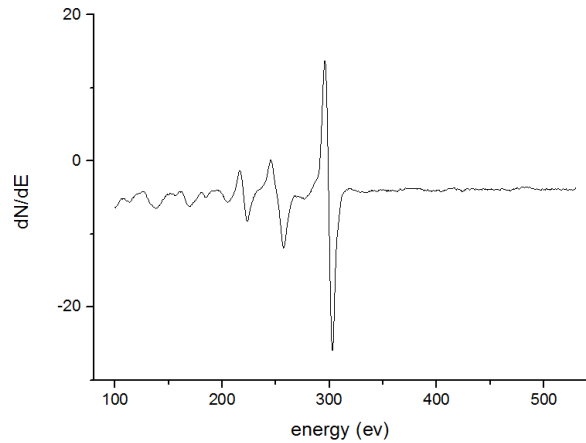


Figure 15: Auger spectrum after cleaning

## II XRR analysis of the sample

While the LEED pattern indicates that the surface is not flat enough, XRR measurement analysis can quantitatively confirm this and enable us to precisely determine surface roughness of the sample. Consequently the sample was mounted in the x-ray laboratory and XRR measurements were done. Specular reflectivity intensity is plotted on a graph in fig. 16.

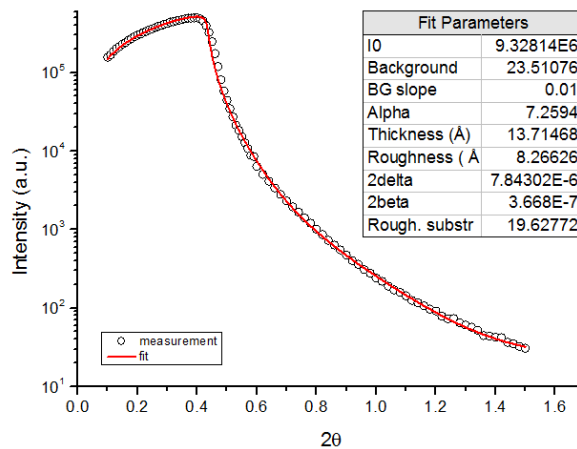


Figure 16: X-ray reflectivity of the sample

Plotting was done in Origin while data fitting was done in Fewlay, a program specialized for analysing surfaces with XRR. Although very efficient with multi-layered substrates, Fewlay can not work with single crystal surfaces (zero layers) and it was therefore necessary to include one layer in the fit. This is not a problem as the surface of the crystal can be considered the layer, and bulk the substrate. The fit is then merely expected to give the parameters of the layer corresponding to the substrate itself.

First of all, what we can see from the measured data is that the sample is quite clean and has no layers of other materials on the surface, since any kind of oscillations, that would be produced by constructive interference between the layers, is absent. First part of the graph, before the critical angle, is dumped. This is only due to geometry of the setup, because the illumination of the sample increases with the increasing angle and is included in the fit under the setup information, so the

fitted curve follows the measurement well even in this regime.

Values for  $\delta$  and  $\beta$  of the layer correspond to values for rhodium obtained from [9], which confirms our assumption that the surface of the sample can be modelled as a layer in Fewlay. From the fit, the obtained roughness of the sample is:  $\sigma = 19.6 \text{ \AA}$ . This is a surprisingly high roughness of a single crystal and explains blurry patterns obtained by LEED.

### III AFM images

As a final confirmation of the roughness of the sample, we scanned its surface in the AFM. The images are shown in fig. 17. Non-uniformity of the sample is now even directly confirmed, so if there were any doubts while interpreting XRR data, the concern is now settled with this direct imaging. From topography we can see the roughness of the surface and from the phase scan, the non-uniformity of the sample. By analysing the images with image editor (fig. 18), the roughness of about 2 nm is obtained, which confirms the XRR measurements.

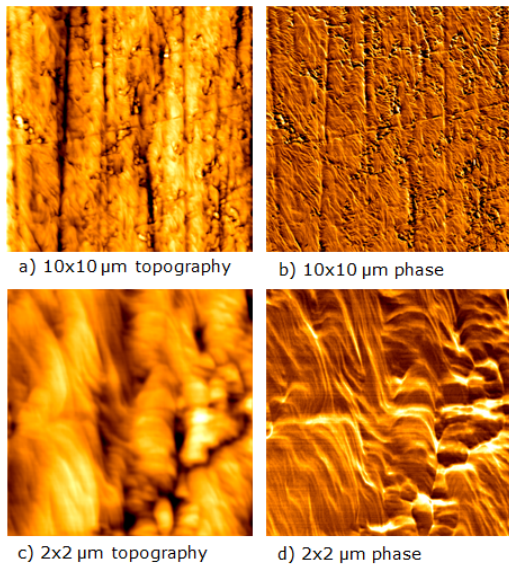


Figure 17: AFM images of the sample

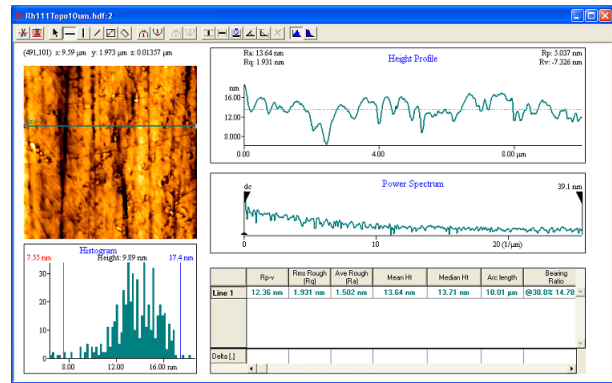


Figure 18: Image analysis

## V Conclusion

In this project the Rh(111) single crystal surface was treated and characterized as a part of the oxidation experiments preparation process. The idea was to make the surface as flat and as uniform as possible in order to minimize any possible side effects arising from defects, dislocations or impurities. Main goal is the future Rh-nanoparticles oxidation kinetics study and for that one needs a detailed study of oxidation of pure rhodium itself, in order to interpret nanoparticles data, compare it with the uniform surface sample and detect phenomena related solely to nanoparticles.

The sample was subjected to 4 cycles of sputtering and annealing with addition of one oxidation annealing after the second cycle. Sputtering and oxidation eliminated foreign atoms, which was confirmed in the Auger spectrum of the cleaned sample. However, the annealing procedure, done at 650-700 °C, was not efficient enough to flatten apparently very rough surface of the sample.

Annealing at even high temperatures should be done to further increase the quality of the surface, which is of paramount importance for the oxidation experiments.

Additional quantitative studies were done with the sample by x-ray reflectivity and atomic force microscopy. Both methods confirmed surprisingly high roughness of about 20 Å. Until flattened to smaller roughness, this crystal should not be used in experiments since its imperfection would complicate data analysis and could even lead to undesired effects.

## Acknowledgements

I would like to thank to the X-ray Physics and Nanoscience group of Deutsches Elektronen Synchrotron for an invaluable experience and knowledge obtained during my summer research in their group. I thank to Dr. Vedran Vonk, Prof. Andreas Stierle, Dr. Thomas F. Keller, Dr. Heshmat Noei and Dirk Franz for all their guidance, help, advice and discussions of my results. And special thanks to Patrick Müller, for discussing with me every step of my project, for his patience in explaining all the methods and demystifying all the complicated equipment.

## References

- [1] P. Holister, J.W. Weener, C. Roman, T. Harper: Nanoparticles, Cientifica, October 2003
- [2] C. Kittel: Introduction to Solid State Physics, 8th ed. Wiley, 2005.
- [3] Low energy electron diffraction - LEED: Presentation prepared by professor Wolfgang Ranke, 2009.
- [4] [http://www.chem.qmul.ac.uk/surfaces/scc/scat5\\_2.htm](http://www.chem.qmul.ac.uk/surfaces/scc/scat5_2.htm)
- [5] j. Als-Nielsen, D. McMorrow: Elements of Modern X-ray Physics, 2nd ed. Wiley, 2011.
- [6] M. Yasaka: X-ray thin film measurement techniques, The Rigaku Journal, 2010.
- [7] <http://www.keysight.com/main/editorial.jsp?ckey=1774141&id=1774141&nid=-33986.0&lc=spa&cc=VE>
- [8] [http://hone.mech.columbia.edu/wiki/doku.php?id=wiki:atomic\\_force\\_microscope](http://hone.mech.columbia.edu/wiki/doku.php?id=wiki:atomic_force_microscope)
- [9] <http://www.cxro.lbl.gov/>